ASTFE
American Society
of Thermal and Fluids Engineers

8th Thermal and Fluids Engineering Conference (TFEC)
March, 26-29, 2023
Partially Online Virtual and at University of Maryland, MD Conference

TFEC-2023-xxxxx

A DYNAMIC ENERGY MODEL FOR DISPLAY CASES CONSIDERING FAULTS IN SUPERMARKETS FOR LOW GWP REFRIGERANTION

Yanfei Li[1*], Jian Sun[2], Zhiming Gao[3], Borui Cui[1]

[1]Grid Interactive Controls Group, Oak Ridge National Laboratory, Oak Ridge, TN 37830, USA
[2]Multifunctional Equipment Group, Oak Ridge National Laboratory, Oak Ridge, TN 37830, USA
[3]Building Equipment Research Group, Oak Ridge National Laboratory, Oak Ridge, TN 37830, USA

ABSTRACT

Display cases are widely used in supermarkets to demonstrate commercial goods for customers, like milk, frozen food, ice-cream, etc. There are two types of display case: open case and closed case. The goods inside display cases need to stay within a stable temperature range to meet the quality standards. However, due to variety of faults (e.g., leaving door opening), it is hard to maintain a stable temperature. The associated energy consumption from display cases is extremely high due to faults. There is a need for a dynamic energy model to accurately predict the good temperature and energy consumption under faults. A dynamic model is developed based on operation data collected through field tests in a low global warming potential (GWP) refrigeration system, at Oak Ridge National Laboratory.

KEY WORDS: Dynamic Energy Model, Display Case, Low GWP Refrigeration, Fault model, Refrigeration System.

NOMENCLATURE

C_{pa} specific heat for air (J/kg-K)
M_a mass of air inside the display case (kg)
T_a air temperature of display case (°C)
U_{az} heat transfer coefficient due to thermal conduction between compartment internal air and ambient (W/m^2-K)
A_{az} overall surface area for thermal conduction between internal air and ambient (m^2)
T_z is the ambient air temperature (°C)
h_{ag} heat transfer coefficient due to convection between compartment internal air and goods (W/m^2-K)
A_{ag} overall surface area for thermal convection between compartment internal air and goods (m^2)
T_g goods temperature (°C)
h_{ae} heat transfer coefficient due to convection between compartment internal air and evaporator average refrigerant temperature (W/m^2-K)
A_{ae} overall surface area for thermal convection between compartment internal air and evaporator surface (m^2)
T_e evaporator average refrigerant temperature (°C)
$\dot{m}_a$ air mass flow rate for the compartment air (kg/s)
C_{pg} goods specific heat (J/kg-K)
M_g mass of the goods (kg)
h_{ainf} heat transfer coefficient due to thermal convection between compartment internal air and infiltration air (W/m^2-K)
A_{ainf} overall surface area for thermal convection between compartment internal air and infiltration air (m^2)

1. INTRODUCTION

*Corresponding Author: liy1@ornl.gov

Based on a market report, there are about 63328 supermarkets in the United States as of 2022[1]. They use display cases for demonstrating goods for customer purchase. There are two types of display cases: closed and open. The closed display case is more for low-temperature goods. It is mainly for frozen foods. The open display case is for fresh goods. It is mainly for fresh vegetables. The refrigeration system is behind those display cases, to provide cooling. Studies show, approximately 50% of the electrical energy consumption is used by refrigeration systems[2] for supermarkets.

Because of the extremely high demands for power, supermarkets produce a considerable amount of global warming potential gas emissions, such as hydrofluorocarbon emissions from leaking of vapor compression cycling and CO2 emissions from electricity originating from power stations [3]. With the increasing requirements of reducing global carbon emissions, there is a demand to increase the efficiency of refrigeration systems and display cases. To reduce the power demands or carbon emissions, there are multiple tracks: (1) Investigating CO2 refrigerants has gained more attention because it has the best global warming potentials compared with traditional refrigerants[4] which are hydrofluorocarbon-based chemical compounds. (2) Improving the efficiency of refrigeration components (e.g., compressor[5–7] and heat exchanger[8–11].) by using efficient materials is another approach. There are abundant research publications on this aspect. (3) Optimizing system efficiency is desired with updated new refrigeration components[12–14]. The typical manner is to couple the vapor compression cycle system and display-case model as a cohesive framework [15,16].

However, available studies on refrigeration systems assume no fault in the component or system. Many studies applied computational fluid dynamics (CFD) techniques to model the display case internal temperature and airflow distributions[17]. They assume the display case is an enclosed space without faults. Faults are common for refrigeration systems [18]. Faults could cause more than 100% power demands[4]. How quantifying the fault impacts the power demands of refrigeration systems remains a challenge. There are some studies on the refrigeration faults, such as over-charging or under-charging[19] for chiller systems. A recent study shows faults are common for commercial heat pump systems [20]. Another study demonstrated five fault models using a grey-box format for CO2 refrigeration systems [4] and display cases, focusing on the supply air temperature and power demands. However, It did not consider the heat dynamics inside the display case. To the best of the author's knowledge, there is no study investigating the dynamic physical models (white-box format) considering faults for display cases of a CO2 refrigeration system. The display case is the energy demand side for refrigeration systems. It moves the thermal load from the goods to the evaporator to be cooled, which demands power from the compressor behind.

This study demonstrates the display-door-open as the fault of the closed display cases, to develop the dynamic energy models. The measurement data for the evaporator is used to integrate the dynamic models of the display case. To connect with the refrigeration cycles, a deep learning model of the compressor is used to predict the power under fault conditions. There are two groups of study: one group is the baseline; the other group is for the fault.

2. METHODOLOGY

2.1 Display Case The display case is an enclosed space to cool the goods inside. The cooling energy is from the upstream source, e.g., evaporator. Behind the evaporator is a vapor compression cycle system (CO2 as refrigerant) with the compressor, condenser, and thermal expansion valve. The refrigeration system is running continuously to move the heat from inside the display case to the outside environment. **Fig. 1** demonstrates the basic internal structure of the display case. In this study we used the closed display case. This study aims to develop the dynamic energy models for the closed display case.

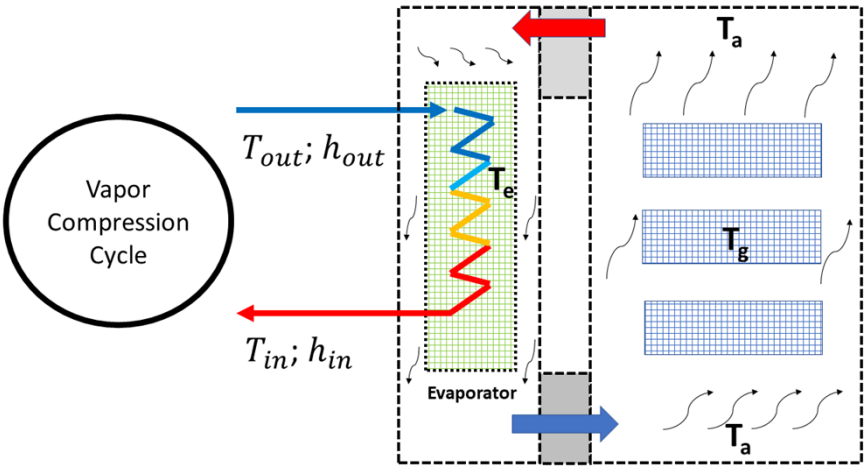

Fig. 1 Display Case Diagram

2.2 Display Case Baseline Model The baseline model is the situation without faults involved. The purpose of the baseline model is to compare against the fault model. The equations are based on the balance of mass and energy, through the lumped parameter manner of using Resistance-and-Capacitance (RC). It is similar to the building/zone thermal model, in which the details are available in the two studies [21,22]. The energy transfer happens among the compartment air temperature (display case internal air temperature), goods temperature, ambient temperature, and evaporator coil surface temperature, due to the temperature difference. Other heat transfer items are ignored in this study (e.g., thermal radiation). In **Fig. 2Fig. 1**, the black arrow indicates the heat flux direction is going from high temperature to lower temperature.

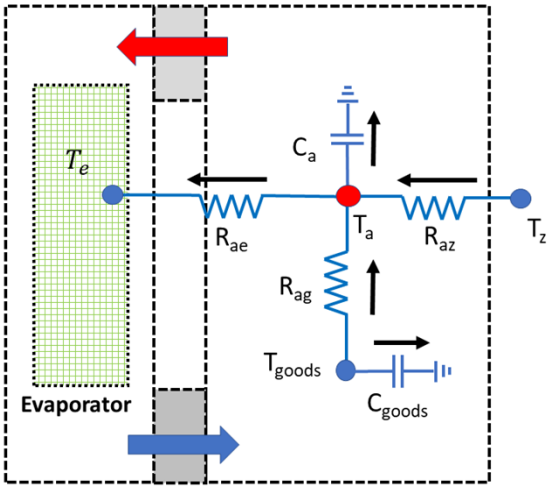

Fig. 2 Display Case Baseline Model

The equations describing the heat transfer are as below:

$$C_{pa}M_a\frac{dT_a}{dt} = U_{az}A_{az}(T_z - T_a) + h_{ag}A_{ag}(T_g - T_a) + h_{ae}A_{ae}(T_e - T_a) \quad (1)$$

$$h_{ag}A_{ag}(T_g - T_a) = C_{pa}\dot{m}_a(T_g - T_a) \quad (2)$$

$$C_{pg}M_g\frac{dT_g}{dt} = h_{ag}A_{ag}(T_g - T_a) \quad (3)$$

In above equations, the compartment air temperature T_a and T_{goods} are the unknown variables need to be solved from the ODE equations. T_e and T_z are obtained from the measurement. All other variables are obtained through literatures[4,15,16,23–26].

2.3 Display Case Fault Model This fault is defined as any behavior or occurrence causing the system or component away from normal operations. Display door open is a common fault. When the display door is open, the ambient air around the display case will be sucked into the compartment for cooling cycles. This is the infiltration, which has higher temperature than the compartment temperature. This leads to higher thermal load which the evaporator coil must move away through heat transfer. Because there is temperature control loop involved to maintain the compartment temperature at certain setpoint. This causes higher compartment temperature which might compromise the quality of goods. The compressor might work at higher/full capacity to meet the thermal load. The demonstration is given in **Fig. 3.**

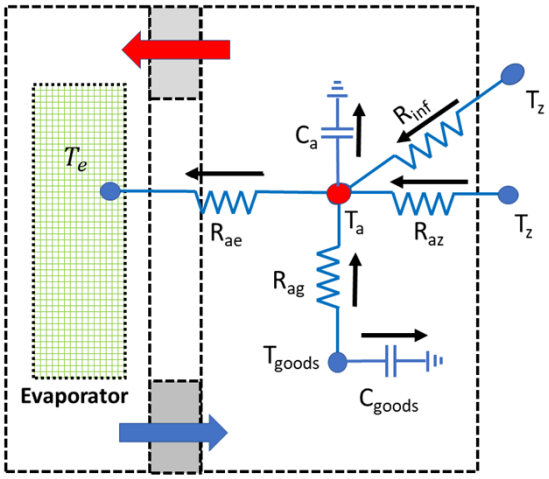

Fig. 3 Display Case Fault Model (Display Case Door Open)

The fault is modeled as the heat convection between the infiltration air and compartment air. The equation describes this fault is shown as below:

$$C_{pa}M_a\frac{dT_a}{dt} = U_{az}A_{az}(T_z - T_a) + h_{ag}A_{ag}(T_g - T_a) + h_{ainf}A_{ainf}(T_z - T_a) + h_{ae}A_{ae}(T_a - T_e) \quad (4)$$

2.4 Data Collection The experiment runs were conducted in the lab environment. The details of the data collection of CO2 refrigeration can be found in the previous studies [27,28].

2.5 Solver The model contains a set of ordinary differential equations (ODE). The DOE solver is from Scipy in Python platform[29].

2.6 Compressor Model We applied the deep learning model to predict the power demands of the compressor. The dynamic energy model of the display case serves as a component to calculate the goods temperature and compartment air temperature, which are inputs to the compressor power calculations. **Fig. 4** shows the flowchart of dynamic energy models and compressors with major impacting input parameters and output parameters. The input parameters are: compartment temperature (T_a), ambient air temperature (T_z), outdoor air temperature (Toa), evaporator average temperature (T_e), goods' temperature (T_{goods}). The output parameter is the power consumption. The deep learning model is based on the PyTorch [30] platform. The dataset is divided into 80% for the training dataset and 20% for the testing data. More details are available in an on-going work for a journal publication.

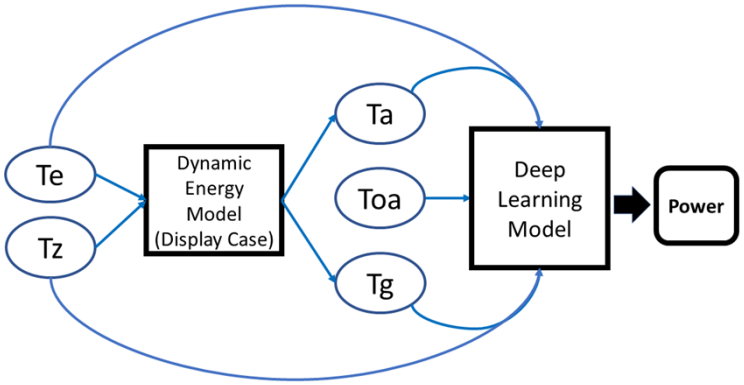

Fig. 4 Compressor Model (Deep Learning)

3. RESULTS AND DISCUSSION

3.1 Goods and Compartment Temperature Under Steady Operations(Ideal) For steady operations in ideal conditions, the initial conditions are T_e = -5 °C and T_g=15 °C . Fig. **5** demonstrates the goods and compartment temperature under steady operations. The steady operations mean the evaporator average temperature (T_e), and ambient temperature (T_z), are constant, which is ideal conditions. The purpose is to show how the goods and compartment temperature change under such ideal conditions. Baseline means the display case is closed without infiltration from the ambient. Fault means the display case with door partially open. The red line is the goods temperature of the baseline. The blue line is the compartment temperature of the baseline. The black dot line is the goods' temperature under fault. The green dot line is the compartment temperature under fault. Those four lines are denoting the calculated values from the dynamic models. From the **Fig. 5**, we can see two interesting patterns:

(a) Baseline scenario: baseline scenario achieves a target temperature (-5 °C) of around 200 seconds. The compartment temperature rises rapidly due to the high initial temperature of goods (15 °C). It rises to the peak value of about 10 °C, and then decreases slowly to the target temperature (-5 °C). This is reasonable because compartment air has smaller thermal capacitance and faster response to the thermal load. Goods temperature has a slower trend compared with compartment temperature due to the higher thermal capacitance. Eventually, the goods temperature also achieves the target temperature.
(b) Fault scenario: Patterns in this scenario are like those in the baseline case. Because of the fault, the compartment temperature and goods temperature achieve the ultimate temperature of around -3 °C. It did not achieve the target temperature of -5 °C. This is because the display door opens too much, which is beyond the maximum cooling capacity of the compressor.

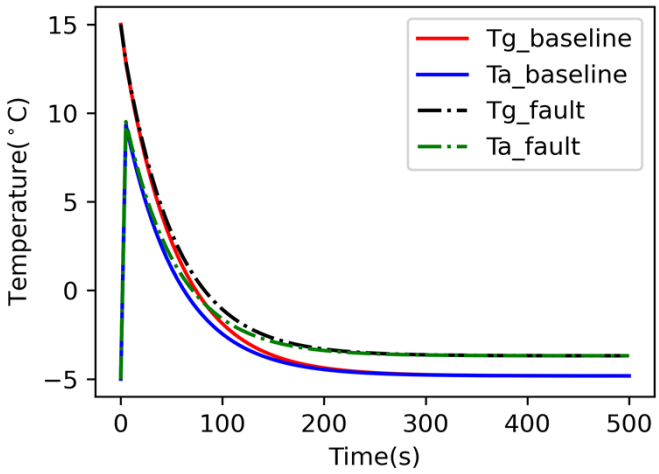

Fig. 5 Temperature Under Steady Operations (Ideal)

3.2 Goods and Compartment Temperature Under Dynamic Operations (Baseline, Field Data)

Actual operations of refrigeration systems are dynamically changing. In this scenario, we plug in the dynamic values of T_e and T_z, into the above equations to solve for the goods temperature and compartment temperature. The solved values are compared against the measurement goods' temperature and compartment temperature (**Fig. 6**). The red line is the goods' temperature with the baseline scenario from the dynamic model. The blue line is the compartment temperature with the baseline from the dynamic model. The black dot line is the measured goods' temperature under fault. The green dot line is the measured compartment temperature under fault. The root-mean-squared error (RMSE) for air temperature is 0.39°C. The RMSE for goods temperature is 6.19°C. **Fig. 7** shows the input variables (ambient temperature and evaporator surface average temperature) to the dynamic models, using the measurement field data.

We can see three major patterns:

(a) Measurements: We can see the measurement has periodic changes, with drastic dynamics. The goods temperature follows along the compartment temperature. The ambient air temperature has drastic changes. The evaporator surface average temperature has periodic cycles.

(b) Model: Similar patterns are observed from the dynamic models for the goods' temperature and compartment temperature.

(c) The goods' temperatures are close between the measurement and model results. The compartment temperature has some discrepancies at some time steps. This indicates there is a need to consider more disturbances in the model (e.g. internal lighting).

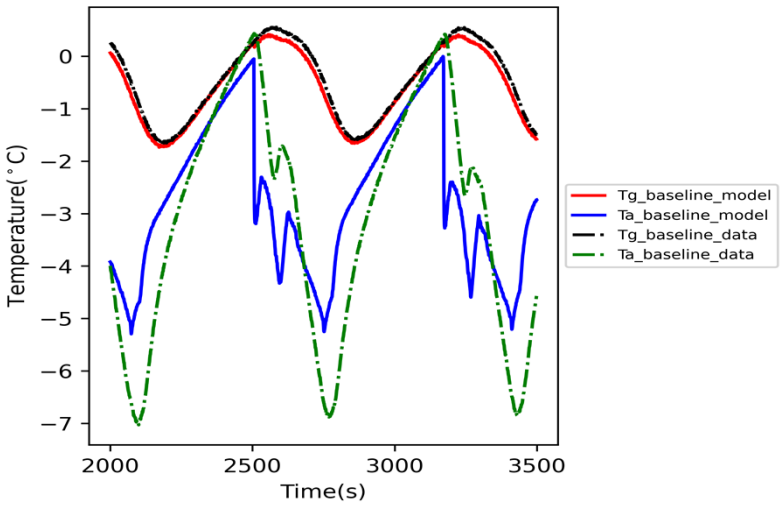

Fig. 6 Temperature Under Dynamic Operations Without Fault

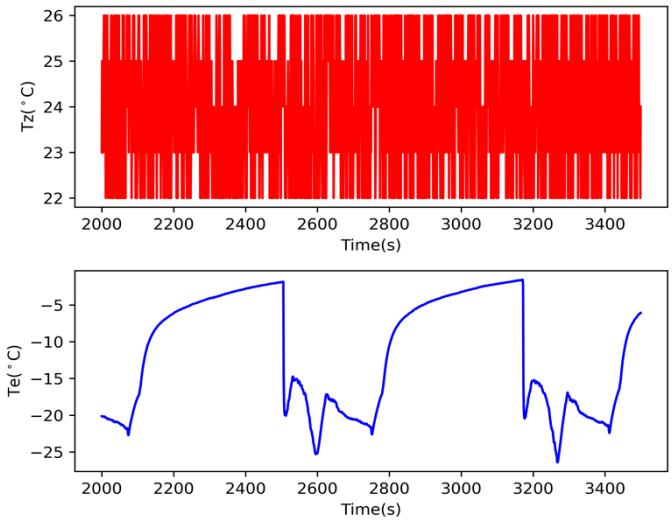

Fig. 7 Input Variables Under Dynamic Operations Without Fault (Field Data)

3.3 Goods and Compartment Temperature Under Dynamic Operations (Under fault, Field Data) The initial conditions are T_a= -18°C and T_g= -18°C . Similarly, we plug in the dynamic values of T_e and T_z, into the above equations to solve for the goods temperature and compartment temperature, under fault scenarios. The solved values are compared against the measurement goods temperature and compartment temperature (**Fig. 8**). The red line is the goods temperature with fault scenario from the dynamic model. The blue line is the compartment temperature with the fault from the dynamic model. The black dot line is the measured goods temperature under fault. The green dot line is the measured compartment temperature under fault. The root-mean-squared-error (RMSE) for air temperature is 3.24°C. The RMSE for goods temperature is 2.51°C. **Fig. 9** shows the input variables (ambient temperature and evaporator surface average temperature) into the dynamic energy model, from the field test data.

We can see three major patterns:

(a) Measurements: The compartment and goods temperature are progressing higher and higher with each cooling cycle, from -18 °C to 15 °C within about 4500 seconds. Each cycle takes about 500 seconds. The goods' temperature follows along with the compartment temperature. The cycle patterns are mainly due to the dynamic ambient air temperature. The upward pattern is due to the increasing evaporator surface average temperature.

(b) Model: modeling results captures the same major patterns as in measurements.

(c) The measurement and model results have a good agreement for the goods' temperature. The compartment temperature still has a bias. This indicates the modeling need to include more terms, such as thermal radiation, internal lighting, etc.

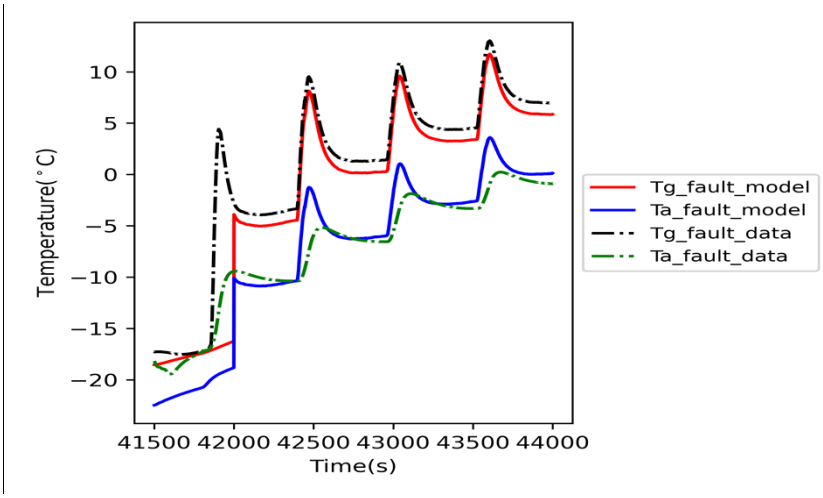

Fig. 8 Temperature Under Dynamic Operations with Fault

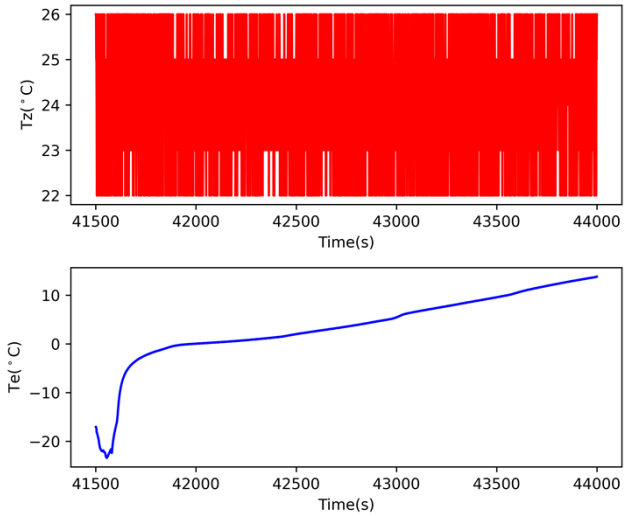

Fig. 9 Input Variables Under Dynamic Operations With Fault (Field Data)

3.4 Power Predictions The **Fig. 10** demonstrated the power demands between measurement and model under selected fault conditions. The Red line denotes the model predictions and the blue line is for the measurement. The prediction shows good agreement (RMSE=0.018).

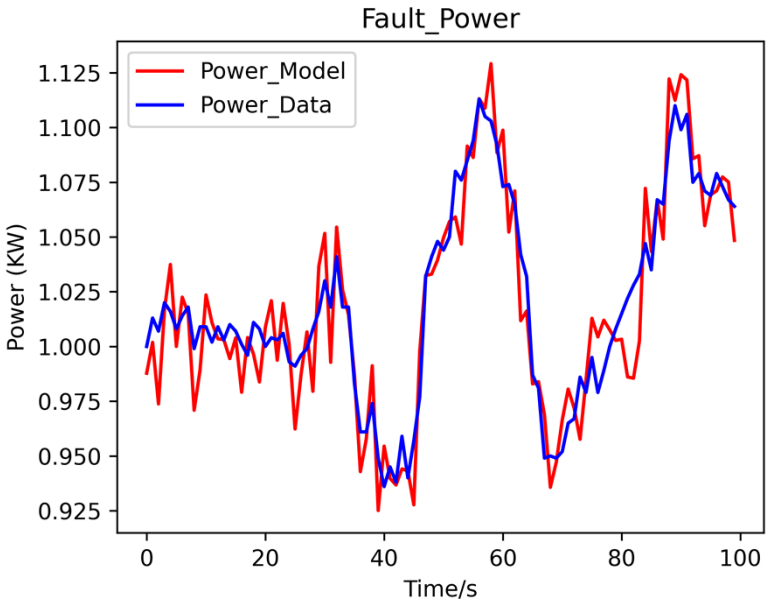

Fig. 10 Power Prediction

4. CONCLUSIONS

This study proposed a dynamic model for the display case for energy prediction purposes. The model demonstrated good agreement between the measurement data and prediction results. (1) For ideal scenarios, under steady operations, the fault strongly impacts the good's temperature and compartment temperature. (2) For actual dynamic operations, the proposed dynamic model can predict the goods' temperature and compartment temperature, with a good agreement through using baseline data and fault data.

There are a couple of items need to be considered in the future work:
(a) Developing the dynamic models with other faults for vapor compressor cycles
(b) Integrating the vapor cycle model with the display case dynamic models, for further study

ACKNOWLEDGMENT

This manuscript has been authored in part by UT-Battelle, LLC, under contract DE-AC05-00OR22725 with the US Department of Energy (DOE). The US government retains and the publisher, by accepting the article for publication, acknowledges that the US government retains a nonexclusive, paid-up, irrevocable, worldwide license to publish or reproduce the published form of this manuscript, or allow others to do so, for US government purposes. DOE will provide public access to these results of federally sponsored research in accordance with the DOE Public Access Plan (http://energy.gov/downloads/doe-public-access-plan)

REFERENCES

[1] IBISWorld - Industry Market Research, Reports, and Statistics n.d. https://www.ibisworld.com/default.aspx (accessed November 18, 2022).
[2] FMI | Supermarket Facts n.d. https://www.fmi.org/our-research/supermarket-facts (accessed November 18, 2022).
[3] James SJ, James C. The food cold-chain and climate change. Food Res Int 2010;43:1944–56.
[4] Li Y, Sun J, Fricke B, Im P, Kuruganti T. Grey-box Fault Models and Applications for Low Carbon Emission CO2 Refrigeration System. Int J Refrig 2022.
[5] Chen Y, Halm NP, Groll EA, Braun JE. Mathematical modeling of scroll compressors—part I: compression process modeling. Int J Refrig 2002;25:731–50.

[6] Chen Y, Halm NP, Braun JE, Groll EA. Mathematical modeling of scroll compressors—part II: overall scroll compressor modeling. Int J Refrig 2002;25:751–64.
[7] Chen Y. Mathematical modeling of scroll compressors. Purdue University; 2000.
[8] Kim B, Lee SH, Lee D, Kim Y. Performance comparison of heat pumps using low global warming potential refrigerants with optimized heat exchanger designs. Appl Therm Eng 2020;171:114990.
[9] Klein SA, Reindl DT, Brownell K. Refrigeration system performance using liquid-suction heat exchangers. Int J Refrig 2000;23:588–96.
[10] Wang Y, You S, Zheng W, Zhang H, Zheng X, Miao Q. State space model and robust control of plate heat exchanger for dynamic performance improvement. Appl Therm Eng 2018;128:1588–604.
[11] Yan Y-Y, Lio H-C, Lin T-F. Condensation heat transfer and pressure drop of refrigerant R-134a in a plate heat exchanger. Int J Heat Mass Transf 1999;42:993–1006.
[12] Baakeem SS, Orfi J, Alabdulkarem A. Optimization of a multistage vapor-compression refrigeration system for various refrigerants. Appl Therm Eng 2018;136:84–96.
[13] Zhao L, Cai W, Ding X, Chang W. Model-based optimization for vapor compression refrigeration cycle. Energy 2013;55:392–402.
[14] Shen B, Rice CK. HVAC system optimization with a component based system model–new version of ORNL heat pump design model. Purdue HVACR Optim. Short Course Int. Compress. Refrig. Conf. Purdue Lafayette USA, 2014.
[15] Gardenghi ÁR. Transient modeling of vapor compression refrigeration systems for domestic applications. Universidade de São Paulo, 2020.
[16] Tulapurkar C, Khandelwal R. Transient lumped parameter modeling for vapour compression cycle based refrigerator 2010.
[17] Cui J, Wang S. Application of CFD in evaluation and energy-efficient design of air curtains for horizontal refrigerated display cases. Int J Therm Sci 2004;43:993–1002.
[18] Li Y, O'Neill Z. A critical review of fault modeling of HVAC systems in buildings. Build. Simul., vol. 11, Springer; 2018, p. 953–75.
[19] Cheung H, Braun JE. Empirical modeling of the impacts of faults on water-cooled chiller power consumption for use in building simulation programs. Appl Therm Eng 2016;99:756–64.
[20] Aguilera JJ, Meesenburg W, Ommen T, Markussen WB, Poulsen JL, Zühlsdorf B, et al. A review of common faults in large-scale heat pumps. Renew Sustain Energy Rev 2022;168:112826.
[21] Li Y, O'Neill Z, Zhang L, Chen J, Im P, DeGraw J. Grey-box modeling and application for building energy simulations-A critical review. Renew Sustain Energy Rev 2021;146:111174.
[22] Cui B, Fan C, Munk J, Mao N, Xiao F, Dong J, et al. A hybrid building thermal modeling approach for predicting temperatures in typical, detached, two-story houses. Appl Energy 2019;236:101–16.
[23] Shafiei SE, Rasmussen H, Stoustrup J. Modeling supermarket refrigeration systems for demand-side management. Energies 2013;6:900–20.
[24] Hermes CJ, Melo C. A dynamic simulation model for fan-and-damper controlled refrigerators 2006.
[25] Ablanque N, Oliet C, Rigola J, Lehmkuhl O, Oliva A. Dynamic Simulation of Household Refrigerators: Numerical Model and Experimental Comparison 2014.
[26] Martinez-Ballester S, León-Moya B, Vesson M, Gonzálvez-Maciá J, Corberán JM. Dynamic performance simulation of a household refrigerator with a quasi-steady approach 2012.
[27] Sun J, Im P, Bae Y, Munk J, Kuruganti T, Fricke B. Dataset of low global warming potential refrigerant refrigeration system for fault detection and diagnostics. Sci Data 2021;8:1–10.
[28] Sun J, Im P, Bae Y, Munk J, Kuruganti T, Fricke B. Fault detection of low global warming potential refrigerant supermarket refrigeration system: Experimental investigation. Case Stud Therm Eng 2021;26:101200.
[29] scipy.integrate.odeint — SciPy v1.9.3 Manual n.d. https://docs.scipy.org/doc/scipy/reference/generated/scipy.integrate.odeint.html (accessed December 20, 2022).
[30] PyTorch. https://www.pytorch.org (accessed December 20, 2022).